Experimental Study of Temperature Distributions Across Two Curtain Wall Systems

Hua Ge
Student Member ASHRAE

Paul Fazio, Ph.D., P. Eng.

Jiwu Rao, Ph.D.

ABSTRACT

Metal curtain walls are widely used in the building industry and offer many advantages including space saving, high quality in manufacturing, light weight, significant aesthetic freedom, and rapid construction. The recent concerns for energy conservation and improved indoor thermal comfort require improvements in their performance. Initially, the metal curtain wall industry grew within the metal window industry, and standards developed for windows are also used to evaluate the performance of curtain walls. However, the heat flow through curtain walls is more complex than in windows and depends to a great extent on the design details. For example, the application of high-performance glazing units to increase the thermal resistance of the envelope can be compromised by the thermal bridges at the joints, such as the fastening screws and the return of back-pans. To evaluate the overall thermal performance of curtain walls accurately, it is necessary to study the complete wall assembly.

An experimental study of temperature distribution across two curtain wall systems is presented in this paper. A two-story full-size specimen (12.5 by 22 ft), incorporating various design details including spacer type, the glazing unit, the thermal break material, and the back-pan design, was tested in an environmental chamber under steady-state and periodic winter conditions. The temperature distributions on glazing panels and at the mullion sections are reported, and the condensation resistance factors for the glazing and the frame are calculated. The results of the preliminary analysis reveal the relative impact of these design details on the performance of the respective curtain wall systems. This is an initial report on the results of this experiment, and additional information will be published as the study proceeds and additional experimental data are analyzed.

INTRODUCTION

Metal curtain walls have been widely used in the building industry since the 1950s due to the ready availability of aluminum as a building material (Ledbetter 1991). This type of building envelope provides the advantages of high-quality control in fabrication and construction, light weight, space saving, and significant aesthetic freedom. However, metal curtain walls are still weak assemblies, due to the high conductivity of metal and glass, and need further study.

A typical curtain wall system consists of glazing units, insulated spandrels, and a frame (Figure 1). The glazing units make up most of the wall assembly. A clear double glazing unit with 0.25 in. (6.4 mm) thick glass pane and 0.5 in. (12.7 mm) air space provides relatively low thermal resistance over the center-of-glass area (R2.04 or RSI 0.36) under CSA (Canadian Standard Association) winter conditions. Once incorporated into a curtain wall system, this glazing area offers even less thermal protection due to the effects of edge-of-glass and metal frame. The spandrel portion usually consists of a metal back-pan filled with insulation and covered with a sheet of glass or other facing materials on the exterior. Although the thermal resistance in the center of the spandrel panel can be sufficiently high, the thermal bridge created by the return of the metal back-pan in the interior significantly reduces the thermal resistance of the assembly. For example, a two-dimensional simulation and experimental test carried out by Carpenter and Elmahdy (1994) found that the thermal conductance at the edge-of-

Hua Ge is a Ph.D. student, **Paul Fazio** is a professor, and **Jiwu Rao** is a research associate at Concordia University, Montreal, Quebec, Canada.

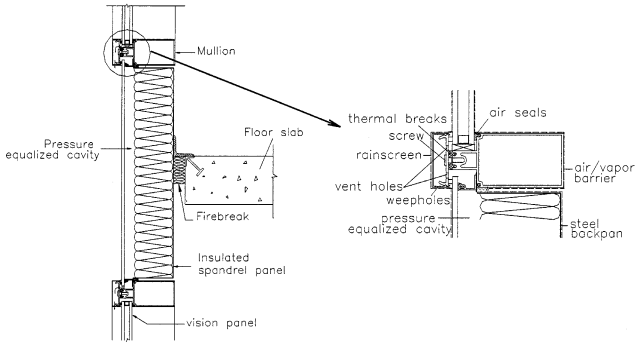

Figure 1 *The cross section of a typical curtain wall.*

spandrel, which is the perimeter area within 2.5 in. (63.5 mm) of the frame, was 7.5 times of that at the center-of-spandrel, and the curtain wall total U-factor was even slightly higher than a standard double-glazed window.

The total thermal conductance of metal curtain walls can be reduced by using high-performance glazing units, such as insulated glazing units (IGUs) with low-E coating, argon or krypton gas filling within the glazing cavity, and "warm" insulating spacers. However, the benefits provided by these high-performance IGUs can be greatly reduced by the performance of mullions and spandrel panels. A simple calculation (EE 1995) on an aluminum curtain wall whose configuration is similar to that shown in Figure 1 has indicated that by replacing the standard double IGU ($U_{center\text{-}of\text{-}glass}$ = 0.49 Btu/h·ft^2·^{o}F or 2.78 W/m^2·K) with high-performance glazing units ($U_{center\text{-}of\text{-}glass}$ = 0.27 Btu/h·ft^2·^{o}F or 1.53 W/m^2·K), the overall thermal conductance is reduced by 19% from U_{total} of 0.48 Btu/h·ft^2·^{o}F (2.73 W/m^2·K) to U_{total} of 0.39 Btu/h·ft^2·^{o}F or (2.21 W/m^2·K), although the high-performance glazing unit provides 55% lower thermal conductance for the center-of-glass. The dimension of the curtain wall assembly calculated is 10.58 by 33.5 ft (3.22 by 0.84 m), in which the glazing panel makes up 56%.

Besides the thermal bridge produced by the metal backpan, the screws used to fasten the wall assembly create another thermal bridge. The effect of this thermal bridge depends on the materials and spacing of screws (Griffith et al. 1998). In addition, the application of pressure equalization rainscreen design in metal curtain walls makes the spandrel adapters and mullion noses exposed to the cold air. The washing effect of cold air at the mullion nose may lower the function of thermal breaks. All of these factors affect the overall performance of metal curtain walls. To accurately evaluate the thermal performance, it is necessary to treat the metal curtain wall as an integrated system instead of just a window assembly. For decades, the U-factor of metal curtain walls has been represented only by the U-factor of the vision panel. The new edition of Canadian Standard A440.2 (CSA 1998) recommends evaluating both the vision panel and the spandrel panel.

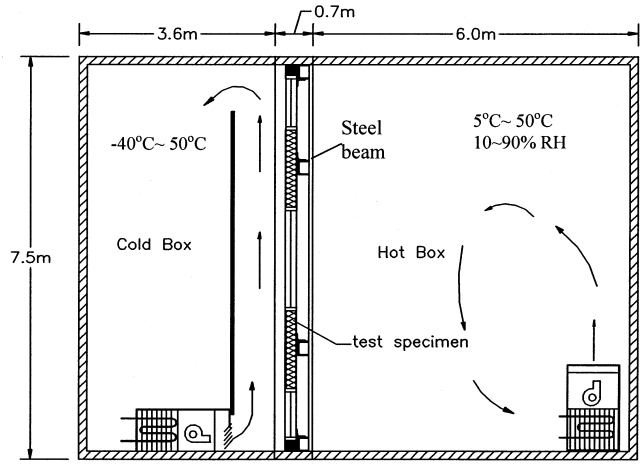

Figure 2 *The experimental setup in the environmental chamber.*

So far, however, no comprehensive study has emerged in our survey, which treats the curtain wall as an integrated system and which considers the impact of the design details on the overall thermal performance of the wall, including energy consumption, impact on thermal comfort, and condensation resistance. In fact, not many studies seem to have been carried out exclusively on curtain walls.

The concern for energy conservation in recent years has led manufacturers to improve the performance of curtain wall systems. High-performance curtain walls are available on the market, but they have difficulty in competing with the "mainstream" products due to the higher cost. By quantitatively demonstrating the benefits of high-performance curtain walls, such as higher energy savings and improved thermal comfort in heating-dominant cold climates, the higher initial cost of high-performance curtain walls would be better justified and market resistance would be reduced.

A research program has been designed to study the overall performance of two types of metal curtain walls. The experimental aspect includes three main areas: air leakage test, thermal performance tests, and measurements of air movement induced by the cold glazing surface. This paper focuses on the initial results of the thermal performance tests. The air leakage test results are reported in Fazio et al. (2001).

EXPERIMENTAL SETUP AND PROCEDURE

Experimental Setup

The experimental study is being carried out on a large-scale curtain wall specimen in an environmental chamber (Figure 2). This facility has been designed to evaluate the overall performance of large-scale building envelope systems under simulated outdoor climatic and indoor environmental conditions. It can accommodate wall specimens of up to 13.5 by 23.5 ft (4.1 by 7.2 m), which is equivalent to approximately two commercial stories or three residential stories. The envi-

ronmental chamber consists of one cold box, one hot box, and one structural frame to accommodate the wall specimen. It can be used in different testing modes: guarded hot box (ASTM 1993), calibrated hot box (ASTM 1996), or a single large environmental chamber. In the last mode, two boxes are joined together without the specimen to form a large chamber for hosting a test hut inside. Several research projects have been carried out using this configuration (Desmarais et al. 1998; Fazio et al. 1998).

Temperature and relative humidity can be controlled to follow the design conditions in both the cold box and in the hot box. The data acquisition system has 400 input and 22 output channels and can measure temperatures, moisture contents, relative humidity, heat fluxes, and other parameters. Data are recorded and stored automatically by a computer. More information about this facility can be found in Fazio et al. (1997).

The test specimen (Figure 3) is designed to incorporate as many different elements as possible to study the impact of design details on the overall thermal performance of metal curtain walls. The overall dimensions of the specimen are 12.5 by 22 ft (3.81 by 6.7 m). It consists of two different types of curtain walls. The first is a standard system, referred to as System A in this paper, and the second is an improved system, referred to as System B. The difference between these two systems includes three aspects. First, with respect to the frame configuration, a much larger thermal break is achieved by using the reinforced nylon in the frame section of System B, while in System A, a thin strip of nylon works as the thermal break. The aluminum mullion is 2.5 in. (63.5 mm) high by 4 in. (101.6 mm) deep. Second, with respect to the glazing panels, all glazing units in System A are double IGUs with 0.25 in. (6.4 mm) clear annealed glass pane, 0.5 in. (12.7 mm) airspace, and a conventional aluminum spacer. System B incorporates clear, double-glazed units with low-e coating (ε = 0.1), 95%/5% argon/air gas filling, and thermally broken aluminum spacers in the middle section. The top and bottom glazing panels are the same as in System A. Third, in respect to the back-pan design in the spandrel panel, the insulated spandrel panel consists of 0.25 in. (6.4 mm) clear annealed spandrel glass, 0.75 in. (19.2 mm) air gap, and 4 in. (101.6 mm) rigid fiberglass insulation. System A uses standard back-pan design, and System B uses improved back-pan design as shown in Figure 4. The detailed configurations of these two systems and the construction details are shown in Figure 4.

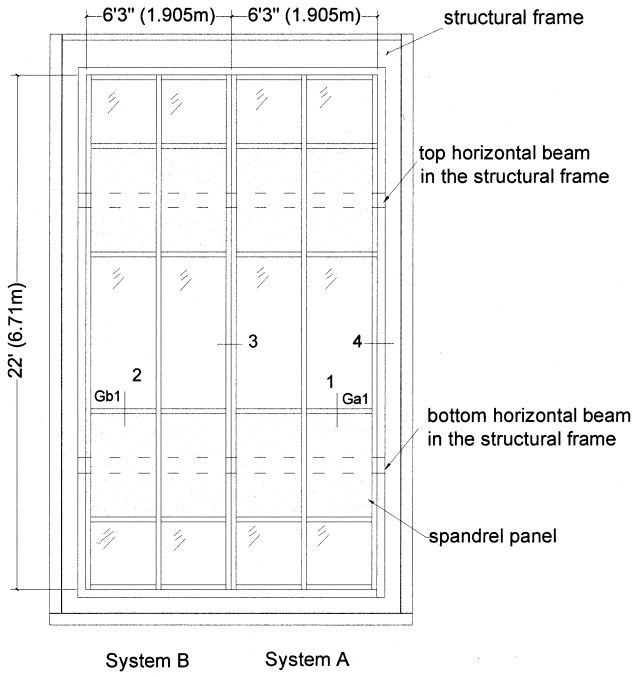

Figure 3 *The configuration of the test specimen (exterior view).*

The test specimen was designed and fabricated by a curtain wall manufacturer. The on-site installation at the laboratory was carried out by a construction team of the company to represent actual workmanship used on site. The construction procedure was divided into two stages to allow the sensor installation in between. To facilitate the installation and to avoid damage to the glazing panels, the main grids and spandrel panels of the test specimen were built up first, outside the environmental chamber. After this step was completed, the structural frame accommodating the curtain wall assembly was lifted by the crane and slowly moved into the space between the cold box and the hot box. The frame was then attached temporarily to the hot box. In the second stage, the installation of insulating glazing units (IGUs), spandrel glass, and pressure plates was carried out in the space between the cold box and the structural frame. After the construction of the test specimen and the installation of all sensors were completed, the structural frame containing the test specimen was lifted and attached to the cold box. Then the movable hot box was closed and sealed onto the structural frame.

Approximately 700 type-T (copper-constantan) thermocouples were installed throughout the test specimen to provide three-dimensional temperature monitoring on the main components of the curtain wall. These thermocouples were premiere grade 30-gauges (NBS special limits of error). The region between the two horizontal beams (Figure 1 and Figure 3) represents one standard floor and is the main part of this study. The installation of the sensors was concentrated in this area. For comparison purposes, the locations of the thermocouples installed on System A were symmetrical to the locations of the thermocouples installed on System B. It should be noted that some heat flow will occur in the plain of the wall at the junction between these two systems because of their different cross sections (Figure 4c). However, this flow was not considered significant for the particular objective of this study.

Thermocouples were installed on the aluminum mullion surfaces, inside mullion channels, and across the mullion section. Thermocouples were also installed on the glazing

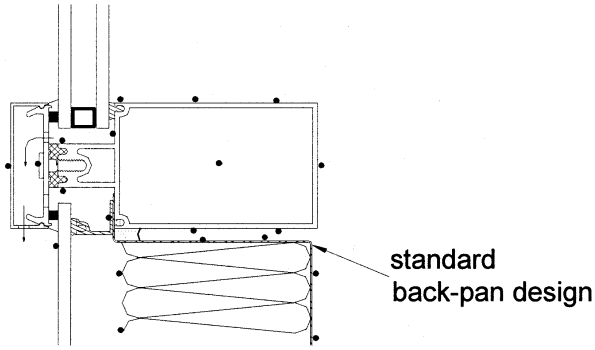

Figure 4a *Section 1: vision sill of System A.*

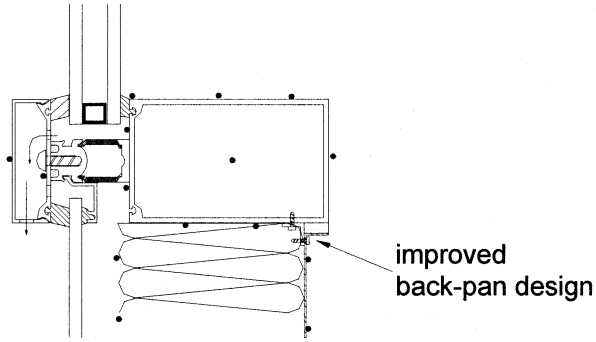

Figure 4b *Section 2: vision sill of System B.*

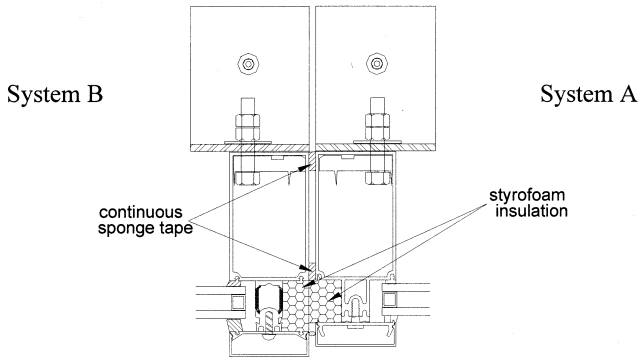

Figure 4c *Section 3: vertical junction of Systems A and B in the test setup.*

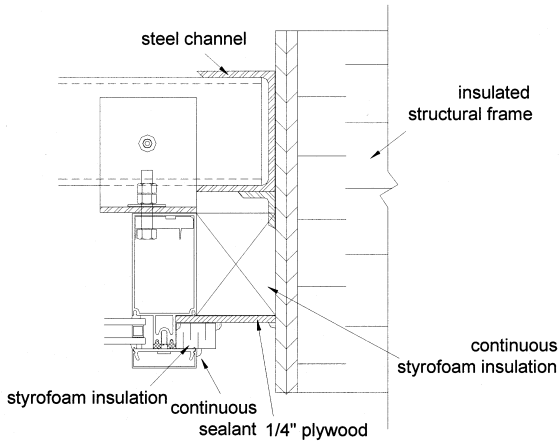

Figure 4d *Section 4: vertical jamb detail.*

Figure 4 *Details of curtain walls tested. (Note: Dots in Figures 4a through 4b indicate the locations of thermocouples.)*

surfaces, spandrel back-pan surfaces, and the exterior surface of the 4 in. (101.6 mm) rigid fiberglass insulation. The sensors on glazing panels were located on both the exterior and interior surfaces. In addition to meeting the requirement of AAMA standard (1998), more thermocouples were added at the edge-of-glass region to monitor the condensation potential (Figure 5). The typical locations of thermocouples across mullions are shown in Figures 4a and 4b. Simulation results from FRAME and the study conducted by Han et al. (1992) were used to determine the locations of thermocouples across the mullion sections.

The inside and outside air temperatures close to the test specimen were measured by thermocouples 3 in. (75 mm) away from the wall surface. These thermocouples were shielded by ϕ.5 in. (12.7 mm) tubes made of aluminum tape to avoid radiation heat exchange with the surrounding. In addition, the temperatures on the baffle surface in the cold box and on the interior wall surface in the hot box were measured. The thermocouples on metal surfaces were attached using aluminum tape. Heat sink compound, a piece of mica, and a piece of clear tape were used underneath each aluminum tape to avoid electrical contact to the metal surfaces. Thermocouples on nonmetal surfaces were attached using construction tape with a drop of heat sink compound to provide a high-quality thermal contact. Since the construction tape has a similar thermal emissivity as the nonmetal surfaces and negligible thermal resistances, the sensor installation would not change the local heat exchange conditions at the specimen surface.

Experimental Procedure

The test specimen was subjected to several steady-state and cyclic winter conditions, as listed in Table 1. The indoor temperature was kept at T_i = 70ºF (21ºC) for all tests. The relative humidity in the hot box was kept below 30% during all the tests. The adoption of the worst condition of –25ºF (–32ºC) is to study the condensation potential of these two different curtain wall assemblies. The cyclic test evaluates the thermal response of metal curtain walls when subjected to the periodic variation of the outside temperature.

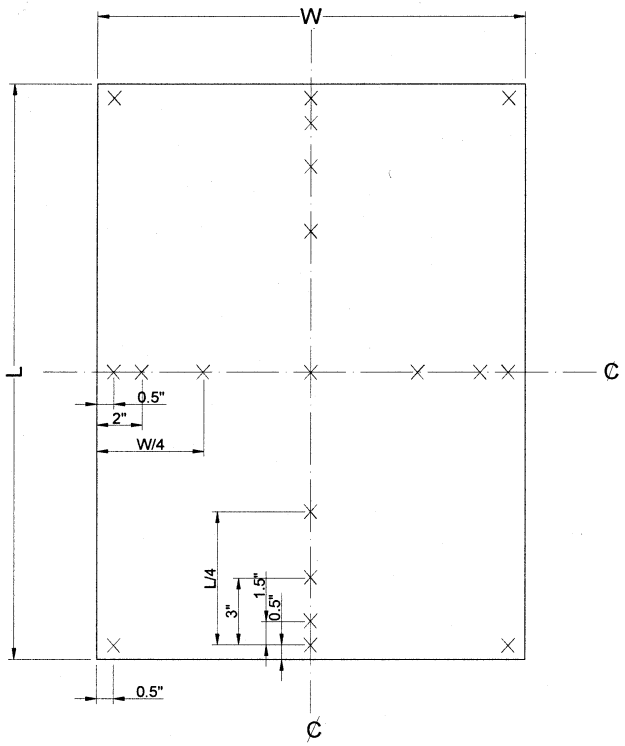

Figure 5 *Thermocouple locations on the glazing surface.*

Each of the tests described above consists of three stages—start-up to reach steady state, maintain steady state, and measurement. It took six to eight hours for the test specimen to start up and reach steady state. The test specimen was allowed to stay in the steady state for 12 consecutive hours before taking measurements. In the last stage, measurements were taken over a period of 12 hours or more. Due to the limitation of the number of channels in the data acquisition system, the sensors for the two systems were read alternately. To ensure the identical test conditions, 12 thermocouples were chosen as the common points and readings were scanned continuously. Those measurements showed that the test conditions subjected by each system were the same. The variations in the measured temperature used for analyses were within ±0.2ºF (±0.1ºC) during the steady-state tests.

EXPERIMENTAL RESULTS AND DISCUSSION

When subjecting the test specimen to the same test conditions, the detailed temperature comparisons can reveal the relative thermal performance of these two curtain wall systems and the impact of their design details. The temperature profiles on curtain wall components and the preliminary analyses are presented below.

Temperature Profiles on Glazing Surfaces

A substantial amount of effort has been made on improving thermal performance of windows and many in the literature have reported the window surface temperatures (Wright 1998; Elmahdy 1996; Griffith et al. 1996; Sullivan et. al. 1996). However, due to the difference in boundary configurations between metal curtain walls and windows, the heat flow pattern may be different at the edge-of-glass region, which is normally the weakest place for condensation. Whereas this study evaluates the overall thermal performance of metal curtain walls as an integrated system, the glazing surface temperatures, especially at the edge-of-glass region were monitored. For completeness, the two-dimensional temperature contours on the interior surface of glazing panel G_{a1} and G_{b1} are presented in Figure 6. These contours were generated based on the measurements under the 0ºF (outdoor) and 70ºF (indoor) (–18ºC/21ºC) test conditions.

TABLE 1
Test Conditions

	Hot box conditions (T_i)	Cold box conditions (T_o)	Remarks
Steady-state tests	70ºF (21ºC)	14ºF (–10ºC)	
		0ºF (–18ºC)	CSA winter condition
		–11ºF (–24ºC)	Montreal design condition (99%)
		–25ºF (–32ºC)	Worst condition—annual extreme daily mean minimum temperature
Cyclic test		–12–6 sin (t/12π) (ºC) 10.4 + 21.2 sin (t/12π) (ºF)	Sinusoidal profile based on weather files from the Montreal weather station

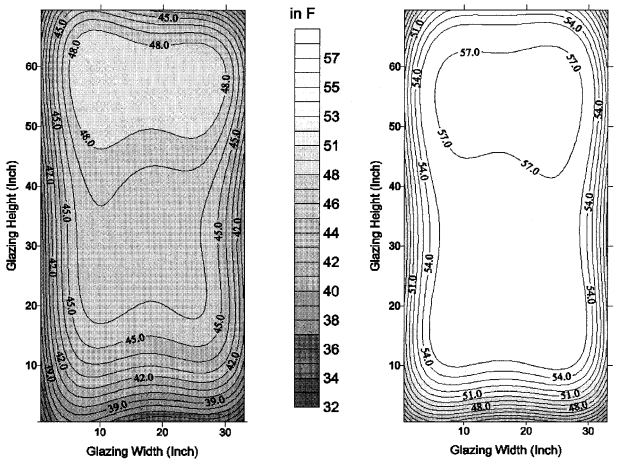

(a) glazing panel G_{a1} (b) glazing panel G_{b1}

Figure 6 *Two-dimensional temperature contour on the interior surfaces of glazing panels under test condition 0ºF (outdoor) and 70ºF (indoor) (–18ºC/21ºC).*

Due to the limited locations of measurements, as shown in Figure 5, these contours can only show the general distribution pattern. Similar findings as the existing studies are formulated. The high-performance glazing panel in System B shows much warmer surface temperatures, which is revealed by the lighter color in Figure 6. Both the surfaces are warmer at the upper part and colder at the lower part due to the convection within the glazing cavity and the effect of spacer. Moreover, the temperatures at the corners of the edge-of-glass regions were lower than those at the center lines. The lower parts, especially the lower corners of the glazing units, are, therefore, most vulnerable to condensation.

Temperature Distribution Through Mullion Sections

Figure 7 shows the temperature distributions across the mullion sections at vision sills under the 0ºF (outdoor) and 70ºF (indoor) (–18ºC/21ºC) test condition. Due to the high-thermal conductivity, the aluminum surface temperature is very sensitive to the local film coefficients. This has been indicated by the temperature difference between the top mullion surface and bottom mullion surface in System A (Figure 7a). The bottom mullion surface is exposed to the return of the back-pan, which has much lower surface temperature than the indoor air, and the air movement is restricted as well; consequently, the local film coefficient is lower. The lower film coefficient results in around 0.9ºF (0.5ºC) lower surface temperature. The aluminum mullion tube works as a fin, and temperature gradient exists along the surface. The temperature gradient in System B is smaller than that in System A due to the much larger thermal breaks, and more uniform mullion surface temperature is achieved. One interesting point worthy of being mentioned is the high-temperature gradient at the return of the steel back-pan, which implies high heat loss through this thermal bridge. At the sill section of System B, the warmest point on the mullion is the right lower corner, which has a temperature of 54.9ºF (12.7ºC). The direct connection with the steel back-pan may be the reason.

In general, the much larger thermal break achieved with the use of reinforced nylon at the frame section of System B results in a 12.6ºF (7ºC) increase in the temperature of the mullion front surface at the vision sill section. The enhanced frame configuration and the shift of the return of the back-pan in System B achieved a 3ºF (1.7ºC) improvement in the surface temperatures of the back-pan. The effect of this back-pan design can be seen in the exterior surface temperatures of the insulation as well. In System A, the exterior insulation surface temperature at the edge-of-spandrel is 4.3ºF (2.4ºC) warmer than that of System B. The lower temperature in System B indicates that the thermal bridge effect is reduced in the improved configuration. The air temperature in the window rabbet is much colder (16.0ºF/–8.9ºC) in System B than that in System A (24.4ºF/–4.2ºC). When the warm and moist indoor air exfiltrates to the cavity, condensation and even frost may be formed. If the weather condition continues, the formed frost may block the weepholes on the pressure plate, and water penetration could occur. Therefore, good airtightness should be maintained. Similar test results are evident for three other steady-state test conditions.

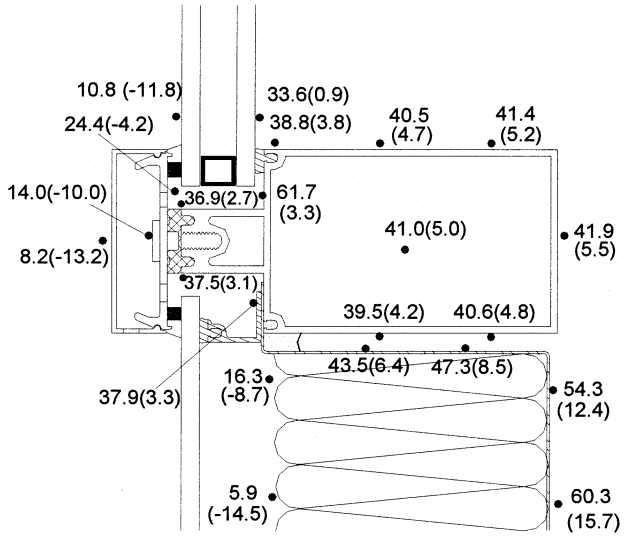

Figure 7a *Section 1: vision sill in System A.*

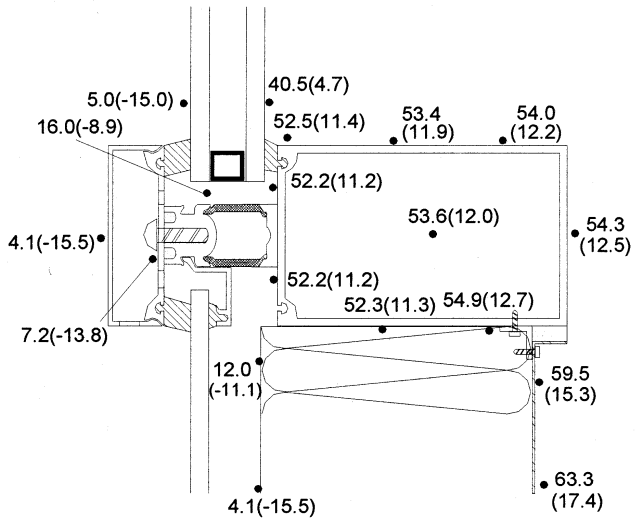

Figure 7b *Section 2: vision sill in System B.*

Figure 7 *Temperature distributions across mullion sections under 0ºF outside/70ºF inside (–18/21ºC) condition. (Note: The values indicated in the drawings are temperatures in degrees Fahrenheit and the values in parentheses are in degrees Celsius.*

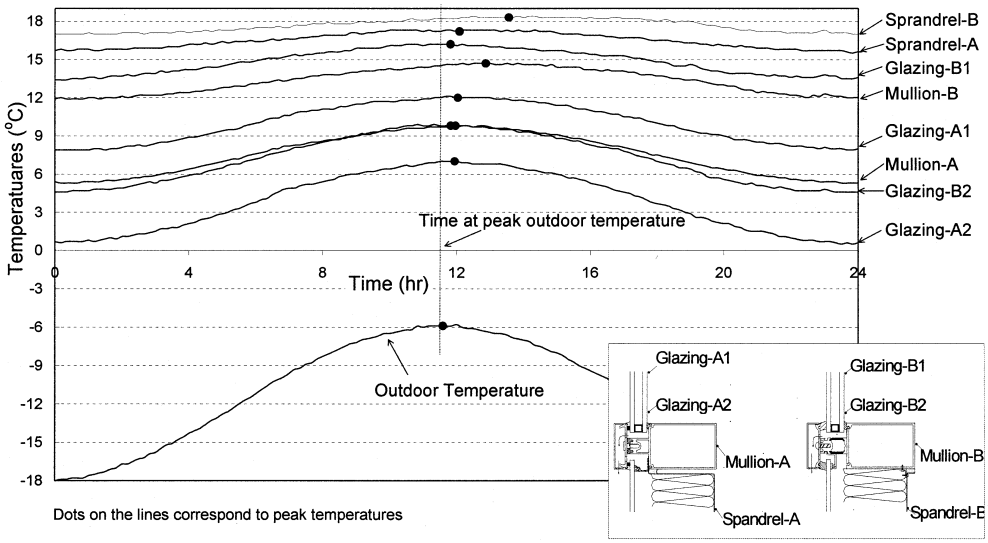

Figure 8 *Thermal responses of curtain wall components to sinusoidal outdoor air temperatures.*

TABLE 2
Measured CRF Under CSA Test Conditions*

Systems	Condensation Resistance Factors	
	CRF_G	CRF_F
System A—Standard	59	61
System B—Improved	72	78

* Notes: In accordance with AAMA, all numbers are rounded to whole numbers.

By comparing these temperatures, it has been found that the edge-of-glass is still the most likely location for condensation to occur. The aluminum frame surface temperature is sensitive to the local film coefficient, and condensation will more likely occur at places where less frame surface is exposed to the room air and where the warm air movement is restricted.

Condensation Resistance Factor (CRF)

The AAMA procedure was followed to calculate the condensation resistance factors (CRFs) for the frame and the glazing. Since this experiment setup is different from the standard test and has different boundary conditions, the calculated results may be different from the standard tests. The calculated results are mainly for relative comparison purposes. The glazing panel G_{a1} in System A, with its surrounding mullions, and the glazing panel G_{b1} in System B, with its surrounding mullions, are considered for the comparison. The calculated CRFs are listed in Table 2. These values indicate that in System A, aluminum frame has a similar condensation resistance as that of glazing panel, while in System B, the condensation resistance of the frame is higher than that of the high-performance glazing panel. In general, the new improved system provides much higher condensation resistance than the standard system.

Thermal Responses Under Cyclic Conditions

Figure 8 presents the measured thermal responses of the curtain wall components to the periodic outdoor temperature. Four representative points were chosen for each system: one at the vision sill mullion surface (Mullion-A, Mullion-B), one at the center of the interior glazing surface (Glazing-A1, Glazing-B1), one at the vertical centerline of the glazing and 0.5 in. (12.7 mm) away from the bottom sight line (Glazing-A2, Glazing-B2), and one at the center of the back-pan surface (Spandrel-A, Spandrel-B).

These measured thermal responses reveal the performance differences between System A and System B. The magnitudes of the temperature variations are listed in Table 3. Components with higher thermal resistance have lower temperature variations. It is found that in each system, the center-of-spandrel has the highest thermal resistance, while the edge-of-glass has the lowest thermal resistance. Each component in System B provides higher thermal resistance than the corresponding component in System A.

The difference in the thermal responses is also evident in the time lag of the selected locations. The time lag at the particular location on the wall is a measure of its delayed temperature response to the outdoor temperature changes. A least squares regression analysis technique has been employed for the estimation. The obtained time lags are listed on the last row in Table 3. Both of the measured temperature response curves and the time lag estimation indicate that the metal curtain wall offers little in term of thermal mass. The time lags to reach temperature peaks after the outdoor air temperature reaches its

TABLE 3a
Temperature Response and Time Lag Under Sinusoidal Outdoor Condition (IP)

Response characteristics	Outdoor air temp.	System A				System B			
		Mullion	Center-of-glass	Edge-of-glass	Center-of-spandrel	Mullion	Center-of-glass	Edge-of-glass	Center-of-spandrel
Max. temp. (^{o}F)	21.2	49.6	53.8	44.6	63.1	58.3	61.2	49.8	65.1
Min. temp. (^{o}F)	-0.4	41.5	46.2	32.9	59.9	53.4	56.1	40.3	62.6
Magnitude (^{o}F)	42.8	36.1	35.8	37.9	33.6	34.5	34.5	36.9	33.3
Time lag (h)		0.37	0.44	0.35	0.49	1.28	0.22	0.23	1.97

TABLE 3b
Temperature Response and Time Lag Under Sinusoidal Outdoor Condition (SI)

Response characteristics	Outdoor air temp.	System A				System B			
		Mullion	Center-of-glass	Edge-of-glass	Center-of-spandrel	Mullion	Center-of-glass	Edge-of-glass	Center-of-spandrel
Max. temp. (^{o}C)	-6.0	9.8	12.1	7.0	17.3	14.6	16.2	9.9	18.4
Min. temp. (^{o}C)	-18.0	5.3	7.9	0.5	15.5	11.9	13.4	4.6	17.0
Magnitude (^{o}C)	6.0	2.3	2.1	3.3	0.9	1.4	1.4	2.7	0.7
Time lag (h)		0.37	0.44	0.35	0.49	1.28	0.22	0.23	1.97

maximum are within half an hour for most of these points. The delays are longer for the interior surface temperatures on the back-pan (Spandrel-B) and on the mullion (Mullion-B) in System B. These longer response delays further demonstrate the reduced thermal bridge effects by a larger thermal break and altered back-pan connection in the improved System B.

CONCLUSIONS

The current research program takes a holistic approach in studying metal curtain wall as an integrated system. The preliminary analysis on experimental data has revealed the impact of design details on the thermal performance of curtain walls. The improved curtain wall system with high-performance glazing units provides higher thermal resistance, warmer surface temperature, and better resistance to condensation. The energy consumption savings and indoor environment improvement offered by the improved system will be quantified with further analysis on the experimental results.

ACKNOWLEDGMENTS

The writers express their appreciation to the Natural Sciences and Engineering Research Council (NSERC) of Canada and the Fonds pour la Formation des Chercheurs et l'aide à la Recherche (Fonds FCAR) of Québec for their financial support and to Kawneer Company Canada Ltd. for providing the design, materials, and installation for the test specimen.

REFERENCES

AAMA. 1998. *AAMA 1503-98*. Voluntary test method for thermal transmittance and condensation resistance of windows, doors, and glazed wall sections. American Architectural Manufacturers Association.

ASTM. 1993. *ASTM C236-89*. Standard test method for steady-state thermal performance of building assemblies by means of a guarded hot box. American Society for Testing and Materials.

ASTM. 1996. *ASTM C976-90*. Standard test method for thermal performance of building assemblies by means of a calibrated hot box. American Society for Testing and Materials.

Carpenter, S., and A.H. Elmahdy. 1994. Thermal performance of complex fenestration systems. *ASHRAE Transactions* 100 (2): 1179-1186.

CSA. 1998. *Energy performance of windows and other fenestration systems*. *CAN/CSA A440.2*. Canadian Standard Association.

Desmarais, G., D. Derome, and P. Fazio. 1998. Experimental setup for the study of air leakage patterns. *Thermal Envelopes VII*. Atlanta: American Society of Heating, Refrigerating and Air-Conditioning Engineers, Inc., pp. 99-108.

Elmahdy, H. 1996. Surface temperature measurement of insulating glass units using infrared thermography. *ASHRAE Transactions* 102 (2): pp. 489-496.

EE (Enermodal Engineering Ltd.). 1995. FRAMEplus toolkit, version 4.0. Enermodal. Kitchener, Ontario.

Fazio, P., H. Ge, and J. Rao. 2001. Measuring air leakage of full-scale curtain wall sections using a non-rigid double

air-chamber method. Submitted to the International Conference on Building Envelope Systems and Technologies (ICBEST). Ottawa, Canada.

Fazio, P., A. Athienitis, C. Marsh, and J. Rao. 1997. Environmental chamber for investigation of building envelope performance. *Journal of Architectural Engineering* 3 (2): 97-102.

Fazio, P., D. Derome, D. Gerbasi, A. Athienitis, and S. Depani. 1998. Testing of flat roofs insulated with cellulosic fiber. *Thermal Envelopes VII*. Atlanta: American Society of Heating, Refrigerating and Air-Conditioning Engineers, Inc., pp. 1-11.

Griffith, B.T., D. Turler, and D. Arasteh. 1996. Surface temperature of insulated glazing units: Infrared thermography laboratory measurements. *ASHRAE Transactions*, 102 (2): pp.479-488.

Griffith, B.T., E.U. Finlayson, M. Yazdanian, and D. Arasteh. 1998. The significance of bolts in the thermal performance of curtain-wall frames for glazed facades. *ASHRAE Transactions* 104 (1): 1063-1069.

Han, H., B.M. Khusinsky, and B. Crooks. 1992. Numerical prediction of moisture condensation on curtain walls using the finite-element method and its experimental validation. *ASHRARE Transactions* 98 (1): pp. 574-583.

Ledbetter, S.R. 1991. A comparative study of the façade industry in the UK, Europe, Japan and the USA. Claverton Down, Bath: Center for Window & Cladding Technology, University of Bath.

Sullivan, H.F., J.L. Wright, and R. Fraser. 1996. Overview of a project to determine the surface temperatures of insulated glazing units: Thermographic measurement and 2-D simulation. *ASHRAE Transactions* 102(2):, pp. 516-522.

Wright, J.L. 1998. A simplified numerical method for assessing the condensation resistance of windows. *ASHRAE Transactions* 104 (1B): pp. 1222-1229.